1-Methyl Naphthalene Reorientation at the Air−Liquid Interface upon Water Saturation Studied by Vibrational Broad Bandwidth Sum Frequency Generation Spectroscopy

Elizabeth L. Hommel and Heather C. Allen*

Department of Chemistry, The Ohio State University, 100 West 18th Avenue, Columbus, Ohio 43210

Received: December 26, 2002; In Final Form: April 18, 2003

Vibrational broad bandwidth sum frequency generation spectroscopy was employed to investigate the surface structure of neat 1-methyl naphthalene (1-MN) and the reorientation of the 1-MN molecules upon saturation of the 1-MN liquid with water. The neat 1-MN liquid molecules have their aromatic rings aligned antiparallel to one another with their methyl groups alternating out of the surface and into the subsurface region from molecule to molecule. With the introduction of relatively few water molecules into the 1-MN liquid (1:336 water/1-MN) a rearrangement of the surface molecules is induced, leading to an increased number density of the methyl groups arranged such that more methyl groups are oriented in the same direction into the air phase at the air−liquid 1-MN interface. Surface tension measurements reveal an increase in the surface tension upon water saturation of the 1-MN liquid, indicating surface activity of the water in the 1-MN solution. It is also clear that the reorientation of the surface 1-MN molecules is reversible.

Introduction

Many organic molecules emitted into the atmosphere partition between the gas and condensed phases in the atmosphere. These molecules can exist either in the particle or liquid phase or possibly as a liquid coating at the surface of solid-phase atmospheric particles. It has been shown that the surfaces of liquid droplets play an important role in the evolution of aerosols in the atmosphere.[1] When a potential reactant collides with the droplet surface, the reactant can diffuse into the drop, react on the surface, or evaporate from the surface.[1−4] Preferred molecular orientations at the surface of such atmospheric aerosols are of interest because aerosol particles will encounter gas-phase water molecules or may react with atmospheric oxidants. The uptake and reaction mechanisms are not well understood on these surfaces.[5] Moreover, aerosol growth and reactivity may be affected by the surface structure if in fact the molecular orientation inhibits, enhances, or in any way alters the reaction pathway.[1,2,6]

Water is among the most abundant trace species in the troposphere, and 1-methyl naphthalene (1-MN), like many small polycyclic aromatic hydrocarbons (PAHs), is prevalent in the lower troposphere of urban regions. In the studies presented here, the air−liquid interface of 1-MN and the bulk 1-MN liquid are investigated; the molecular structure of the air−1-MN liquid interface is investigated before and after water saturation. The result from this study indicates that the surface structure of a hydrophobic solution such as 1-MN or possibly that of an atmospheric aerosol can be dramatically altered by small amounts of adsorbed and/or absorbed water.

Alkyl naphthalenes are common constituents of urban atmospheres. Measurements of gas-phase methyl naphthalenes have indicated that these molecules exist in significant concentrations up to 700 ng/m^3.[7,8] Measurements of particulates using standard collection methods have shown that three-ring and larger PAHs, with correspondingly lower vapor pressures, are the primary

species in PAH-rich particulates[9−12] and that alkyl naphthalenes exist primarily in the gas phase because of their relatively higher volatility. However, partitioning of molecules between the gas and the particle phase is dependent upon the compound's vapor pressure, the atmospheric aerosol number density, and the sizes of organic aerosols present as well as the ambient temperature.[13,14] Alkyl naphthalenes are difficult to quantify in the particulate phase because these semivolatile species can vaporize into the gas phase during and/or after particulate collection prior to chemical analysis. Despite this, there are a few observations of naphthalenes and alkyl naphthalenes associated with the particulate phase of atmospheric aerosols. These studies have identified alkyl naphthalenes including 1-MN in aerosols collected from traffic tunnels in Sweden[15] in addition to dustfall samples in Macao, China.[16]

PAHs, which include alkyl naphthalenes, are commonly introduced into the environment from a variety of fuel sources,[9,17−21] diesel fuel exhaust being a major source.[17−19] The unburned components of the diesel fuel contribute to these exhaust emissions in addition to other aromatic hydrocarbons, which are emitted as partially combusted diesel fuel. 1-MN is a constituent of diesel fuels, and its emission is therefore thought to be due to incomplete combustion of the diesel fuel in light- and heavy-duty diesel vehicles.[18] 1-MN has also been measured in the emissions collected from the tailpipes of gasoline-powered vehicles[9] and in significant concentrations in oceanic regions contaminated by crude oil, for example, the 1989 Exxon Valdez oil spill in the Gulf of Alaska[20] as well as the 1991 Gulf War oil spill along the Saudi Arabian coast.[21]

In the atmosphere, 1-MN and other alkyl naphthalenes are precursors to mutagenic nitro-methyl naphthalenes and are therefore of concern for health-related reasons.[22] Recent studies have also shown a correlation between PAH particulates (diameters <2.5 μm) and chronic respiratory disease, lung cancer, and cardiopulmonary disease.[23−26]

1-MN is a low molecular weight PAH that exists as a liquid at ambient conditions. Its Henry's law constant and vapor pressure are 45 Pa·m^3/mol for aqueous solutions and 8.84 Pa

* Corresponding author. E-mail: allen@chemistry.ohio-state.edu.

10824 *J. Phys. Chem. B, Vol. 107, No. 39, 2003*

Hommel and Allen

(0.066 Torr) at 25 °C, respectively.[22] Gas-phase reactions of 1-MN with NO_2 in the presence of OH or NO_3 radicals have been shown to nitrate the naphthalene ring, leading to the formation of mutagenic methyl nitro-naphthalenes.[27,28] The atmospheric lifetimes of gas-phase 1-MN due to reactions with the OH radical, NO_3 radical, and O_3 are 2.8 h, 250 days, and greater than 125 days, respectively.[22,28] In the studies presented here, we investigate the reorientation of 1-MN at its air−liquid interface after water saturation because water is an abundant component of the troposphere. Any reorientation of the 1-MN at the air−liquid interface may play a role in heterogeneous reaction pathways, which will likely be quite different relative to the gas-phase chemistry of 1-MN.

Sum Frequency Generation Background. Broad bandwidth sum frequency generation (BBSFG) and Raman spectroscopy are used to investigate the surface and the bulk structure of 1-MN solutions, respectively. The nonlinear optical surface technique, BBSFG, utilized in these studies is sensitive to the molecular arrangement at an interface. Because the surface selectivity and the sensitivity to molecular arrangement and specifically the surface orientation are of primary interest in these studies, a brief introduction to the theory of vibrational sum frequency generation (SFG) is given.

SFG spectroscopy is a second-order nonlinear optical technique where the macroscopic nonlinear susceptibility, $\chi^{(2)}$, is probed and only environments lacking inversion symmetry will give rise to SFG. As a surface-sensitive spectroscopic technique, SFG has been used to study a variety of surfaces and interfaces relevant to surface science.[29−36] More recently, SFG has been applied to study solid and liquid surfaces of atmospheric relevance.[37−42] The theory of SFG has been described previously.[43−50] The SFG intensity, I_{SFG}, is shown in eq 1 where the intensity is proportional to the absolute square of the macroscopic nonlinear susceptibility, $\chi^{(2)}$, and the intensity of both the 800-nm and the infrared beams.

$$I_{SFG} \propto |\chi^{(2)}|^2 I(\omega_{IR}) \, I(\omega_{800}) \tag{1a}$$

$$|\chi^{(2)}|^2 = |\chi^{(2)}_{NR} + \sum_v \chi^{(2)}_v|^2 \tag{1b}$$

The nonlinear susceptibility can be described using both a nonresonant term, $\chi^{(2)}_{NR}$, and the sum of the resonant terms, $\chi^{(2)}_v$. The resonant response dominates the nonlinear susceptibility when the frequency of an incident infrared beam, ω_{IR}, is resonant with the v vibration in the system and a SFG intensity enhancement is observed. The resonant macroscopic nonlinear susceptibility, $\chi^{(2)}_v$, is shown in eq 2

$$\chi^{(2)}_v \propto \frac{A_v}{\omega_v - \omega_{IR} - i\Gamma_v} \tag{2}$$

where A_v is the strength of the vth transition moment and the sign of A_v indicates whether a transition is 90° out of phase with respect to the other transitions or if two transition moments exist on opposite sides of the interface. The center frequency of the transition moment is represented by ω_v, and the half-width at half-maximum (hwhm) of the transition is Γ_v. The amplitude, A_v, includes both the Raman and the infrared contributions; therefore, the SFG is observed only when the vibrational transition is both Raman and infrared active. To illustrate this point further, the molecular susceptibility, $\beta_{lmn,v}$,

can be described by eq 3

$$\beta_{lmn,v} = \frac{\langle g|\alpha_{lm}|v\rangle\langle v|\mu_n|g\rangle}{\omega_{IR} - \omega_v + i\Gamma_v} \tag{3}$$

where $\langle g|\alpha_{lm}|v\rangle$ represents the Raman transition moment and $\langle v|\mu_n|g\rangle$ represents the IR transition moment for the molecule. An Euler angle transformation relates the molecular coordinate system (l, m, n) to the laboratory coordinate system (I, J, K).[48−50] The transformation is shown in eq 4

$$\beta_{IJK,v} = \sum_{lmn}\mu_{IJK/lmn}\beta_{lmn,v} \tag{4}$$

where $\mu_{IJK/lmn}$ is the Euler angle transformation between the laboratory coordinates (I, J, K) and the molecule coordinates (l, m, n). The macroscopic susceptibility, $\chi_{IJK,v}$, can be calculated from the molecular susceptibility, $\beta_{IJK,v}$, as shown in eq 5

$$\chi^{(2)}_{IJK,v} = N\langle\beta_{IJK,v}\rangle \tag{5}$$

where $\chi_{IJK,v}$ is equal to the number density, N, multiplied by the orientational average of $\beta_{IJK,v}$.

Experimental Section

Long-established vibrational SFG experiments[51] are accomplished by combining a narrow bandwidth visible laser pulse with a narrow bandwidth infrared laser pulse. The infrared beam is scanned across the vibrational region of interest, and the vibrational spectrum arises when the infrared photons are resonant with an infrared- and Raman-allowed transition of the molecules at the surface and the SFG response is recorded. In the present study, femtosecond broad bandwidth technology is employed. The BBSFG system utilizes a broad bandwidth IR beam ($\sim$600-cm^{-1} bandwidth, $\sim$100-fs pulse duration) rather than a narrow bandwidth IR beam as is used in scanning SFG technologies. Therefore, scanning of the infrared frequency is not necessary. As a result, the vibrational SFG spectrum can theoretically be obtained within one laser pulse.

Instrumentation. The laser system used to obtain the broadband sum frequency generation spectra has been previously described.[29,39,52,53] The laser system used for the BBSFG experiments includes two regenerative amplifiers (Spectra Physics (SP), Spitfires). The amplifiers are seeded with sub-50-fs, 800-nm pulses from a Ti:sapphire oscillator (SP, Tsunami). The amplifiers are pumped using a Nd:YLF (SP, Evolution 30) laser operating at a kHz repetition rate. One of the amplifiers produces 85-fs, 800-nm broadband pulses ($\sim$300 cm^{-1}). The resulting pulses then pump an optical parametric amplifier (SP, OPA-800C) to produce a broadband infrared beam ($\sim$600 cm^{-1}, kHz) for the BBSFG experiments. The second amplifier is equipped with a mask that spectrally narrows the pulse (17 cm^{-1} and $\sim$2 ps). To further narrow the pulse spectrally, an additional mask was added to the compressor within this amplifier, resulting in $\sim$5-cm^{-1} spectral-width pulses.[39] The infrared pulse energy was 10 μJ, and the visible pulse energy was 115 μJ for this experiment. The infrared and the 800-nm beams were overlapped spatially and temporally on the liquid surface of interest. The resultant sum frequency entered the 500-mm monochromator with the entrance slit fully open for high throughput. Thus, the monochromator resolution is limited by the beam waist of the focused SFG beam as it passes through the entrance slit. The spectrum was dispersed spectrally in the monochromator using a 1200 g/mm diffraction

1-Methyl Naphthalene Reorientation

J. Phys. Chem. B, Vol. 107, No. 39, 2003 **10825**

grating blazed at 750 nm (Acton Research, SpectroPro 500i), and the dispersed sum frequency light was collected with a liquid-nitrogen-cooled CCD camera (Roper Scientific, LN400EB, 1340×400 pixel array, back-illuminated CCD). The BBSFG spectra were obtained during 5-min acquisitions, and three spectra were averaged.

Calibration of the BBSFG system was completed by using a BBSFG spectrum of GaAs obtained with the IR beam attenuated by passing it through a polystyrene thin film prior to beam overlap on the GaAs. The resultant infrared beam is structured due to absorption by the polystyrene film, which leads to a structured nonresonant BBSFG spectrum. The peak positions (dips) in the calibration GaAs BBSFG spectrum are used to calibrate the BBSFG system. Thus, calibration of both the IR beam and the detection system is accomplished.

Prior to collecting the BBSFG spectra from the solutions of interest, a nonresonant BBSFG spectrum from the surface of a GaAs crystal was obtained during each experimental session. The BBSFG spectra, which are then normalized with the GaAs spectrum, show a central region where the peaks are easily discernible above the noise. As one would expect, the edges of these normalized spectra are dominated by noise. The normalized spectra are fit using a Lorentzian profile, and only the central region is used for data presentation.

The Raman spectra were obtained by using 45 mW from a 532-nm continuous wave laser (SP, Millennia II), a 500-mm monochromator (Acton Research, SpectroPro 500i; 600 g/mm grating blazed at 1 μm), and a liquid-nitrogen-cooled CCD camera (Roper Scientific, LN400EB, 1340×400 pixel array, back-illuminated and deep depletion CCD). The Raman spectra were obtained when the backscattered light was collected using a fiber optic probe (Inphotonics, RP 532-05-15-FC). The collection fiber optic was coupled to the entrance slit of the monochromator. The slit width was set to 50 μm, and the resulting spectral resolution was 4 cm^{-1}. The Raman spectra were acquired during 2-s exposures to the CCD.

Chemicals. 1-Methyl naphthalene (1-MN) was obtained from Acros Organics with a purity of 97% ($\leq$3% 2-MN) and was used as received because it is nonhygroscopic. Ultrapure water having a resistivity of 18.2 MΩ·cm was also used. The water-saturated 1-MN solutions were prepared by placing approximately equal volumes of water and 1-MN in a glass container, which was vigorously agitated, sealed, and then allowed to settle overnight. The solubility of water in 1-MN is 0.0377 g in 100 g of 1-MN at 20 °C.[54] The 1-MN phase of the water-saturated 1-MN solution was extracted for use in these experiments using a 10-mL syringe. The partially dehydrated 1-MN solution was prepared by placing a vial containing the water-saturated 1-MN phase in a boiling water bath for approximately 2−3 h.

Results and Discussion

The Raman and surface BBSFG spectra of 1-methyl naphthalene (1-MN) are presented in Figures 1 and 2. The Raman spectrum of neat 1-MN, the Lorentzian fit, and the peaks from the deconvoluted spectral fit (Igor Pro 4.05A) are shown in Figure 1. A comparison of the fits calculated using the Voigt profile and the Lorentzian profile were made, and the Lorentzian profile fit the Raman data more effectively. The peak positions were obtained directly from the Lorentzian peak fits.

The Raman spectrum reveals several peaks in the CH stretching region. The assignments of these peaks were accomplished by considering peak assignments from toluene[55,56] and infrared results published for 1-MN.[57,58] Methyl bending
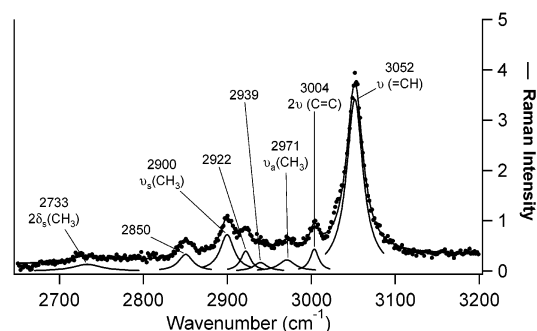

Figure 1. Neat 1-methyl naphthalene Raman spectrum (data points) with a Lorentzian peak profile and the deconvoluted peaks. $2\delta_s$ represents the overtone of the methyl symmetric bending mode, v_s is the methyl symmetric stretch, v_a is the methyl asymmetric stretch, $2v$ (C=C) is the overtone of the carbon/carbon stretching mode, and v (=CH) is the aromatic C−H stretching mode.
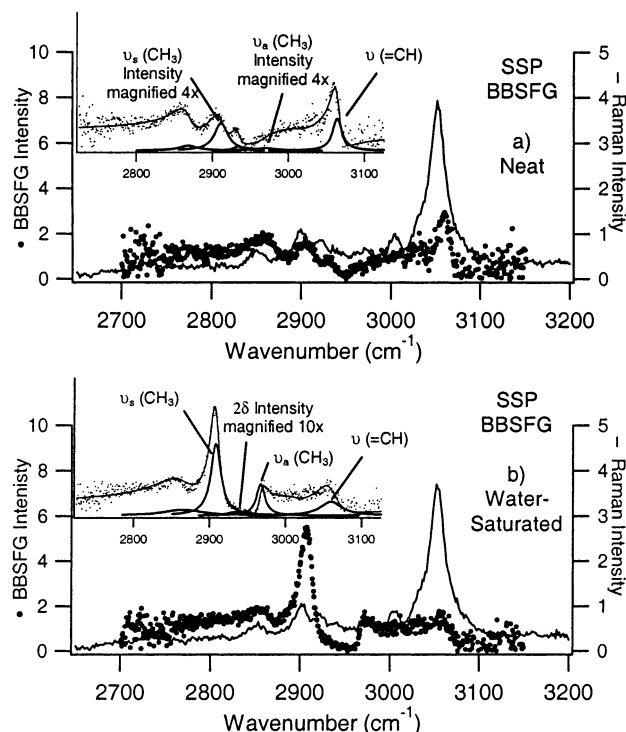

Figure 2. Solid lines in the main figures are the Raman spectra, and data points are the surface SSP BBSFG spectra of (a) neat 1-methyl naphthalene and (b) water-saturated 1-methyl naphthalene. The Lorentzian peak fits for each of the BBSFG spectra are shown as solid lines in the inset. The inset in (a) has both the symmetric (v_s) and the asymmetric stretching (v_a) peaks expanded 4× for clarity.

overtones and the aromatic CH stretching overtones also occur in the aliphatic CH stretching region. Furthermore, there is evidence of splitting of the symmetric stretching mode of the methyl group for the 1-MN molecule.[58] The peaks observed at 2733 and 2850 cm^{-1} are assigned to an overtone of a methyl bending mode and a combination band, respectively. The peak observed at 2900 cm^{-1} is assigned to the methyl symmetric stretching (SS) mode, and the peak observed at 2922 cm^{-1} is assigned to an overtone of a methyl bending mode in addition to the methyl SS. The peak observed at 2939 cm^{-1} is attributed to the overtone of an aromatic C=C stretching mode convoluted with a CH$_3$ asymmetric stretching (AS) mode, and the peak observed at 2971 cm^{-1} is assigned to a CH$_3$ AS mode. The peak observed at 3004 cm^{-1} is assigned to an overtone of the aromatic C=C stretching mode, and the large peak at 3052 cm^{-1} is assigned to the aromatic C−H stretching modes.

The BBSFG spectrum, $S_{SFG}S_{vis}P_{IR}$ polarized, of neat 1-MN is shown in Figure 2a with the Raman spectrum (solid line) from Figure 1 superimposed. The fitting program used to fit this spectrum was written as a separate routine within Igor 4.05A to account for the coherent nature of the SFG spectrum. The data were fit using both a Lorentzian line shape and a Voigt line shape. The results using the Lorentzian line shape more accurately described the BBSFG data. Therefore, the fits shown in the inset of Figure 2a are Lorentzian profiles. The peak positions were taken from the calculated fits, and the vibrational assignments were based on the Raman peak assignments as discussed above. The peaks at 2865, 2908, 2932, and 2967 cm^{-1} are assigned to an overtone of the methyl bending mode, a methyl symmetric stretching mode, another bending mode overtone, and a methyl asymmetric stretching mode, respectively. The splitting of the CH$_3$ SS mode in the Raman spectrum collapses to one CH$_3$ SS peak in the BBSFG spectrum. The aromatic peaks discerned at 3010 and 3061 cm^{-1} are attributed to an overtone of the C=C stretching mode and the CH stretching mode, respectively. The CH$_3$ AS mode at 2967 cm^{-1} is 90° out of phase with the other peaks in this spectrum and is shown in the inset of Figure 2a. The real portion of the nonresonant (NR) contribution is in the same phase as the CH$_3$ AS stretch and is therefore 90° out of phase with the other vibrational modes, and the imaginary portion is out of phase from the real component of the NR SFG response.

The peak positions of the vibrational modes of the surface 1-MN molecules shown in Figure 2a do in fact differ from the peak positions observed for the corresponding modes from the Raman spectrum. However, these BBSFG peak positions are typically within 10 cm^{-1} of the Raman peak positions. (This is also true when comparing the Raman spectrum to the infrared spectrum of 1-MN.[57,58]) As one might expect, there are observed differences between the Raman spectrum and the BBSFG spectrum (Figure 2a) given that the Raman data describes the bulk environment and the BBSFG data describes the surface environment. Furthermore, the BBSFG is a coherent spectroscopy that gives rise to differences in the appearance of the BBSFG spectrum due to interference effects.[45,59]

BBSFG spectra also reveal information about the orientation of the surface molecules. The p-polarized infrared beam used in the SSP polarization combination has an infrared electric field vector component perpendicular to the surface plane, thus the transition moments perpendicular to the surface can efficiently interact with the electric field of the infrared pulse. The transition moment for the aromatic CH stretching is contained in the plane defined by the naphthalene ring system. The transition moment for the CH$_3$ SS is aligned along the methyl group and is contained in the naphthalene plane, whereas the transition moment for the CH$_3$ AS has a component perpendicular to the CH$_3$ SS. The fact that the CH SS and the CH$_3$ SS modes are observed in the SSP-polarized BBSFG spectrum shown in Figure 2a indicates that the 1-MN molecules do not lie flat in the plane of the interface. Yet, these molecules are tilted relative to the surface. Recall from the SFG theory that the SSP-polarized BBSFG signal response is determined by both the orientation of the surface molecules and the surface number density. The observed peak areas in the BBSFG spectrum of Figure 2a are relatively low even though the surface number density is high; the orientation of the 1-MN molecules contributes to the observed BBSFG spectral shape and response. Drozdowski found using X-ray diffraction of the bulk 1-MN liquid that the molecules tend to stack on top of one another with the methyl groups on alternating sides of the stack such
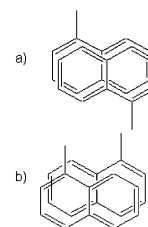

Figure 3. Proposed stacking of the 1-methyl naphthalene molecules at the surface of (a) neat 1-methyl naphthalene and (b) water-saturated 1-methyl naphthalene. The plane of the surface is perpendicular to the aromatic rings.

that the dipoles of the 1-MN molecules are aligned antiparallel as shown in the schematic of Figure 3a.[60] The surface of the neat 1-MN may also be arranged in a similar manner, which is inferred from the relatively low BBSFG signal strength from the CH$_3$ SS mode. However, the fact that we observe a BBSFG response indicates that the CH$_3$ moieties experience a different environment when exposed to the air than the CH$_3$ groups experience when buried in the liquid side of the interface. An ensuing polarizability change could enhance the observation of this extended dimer-like system in the stacking conformation with some tilt angle relative to the surface normal.

The Raman and the surface $S_{SFG}S_{vis}P_{IR}$-polarized BBSFG spectra of the water-saturated 1-MN are shown in Figure 2b. The water-saturated 1-MN solution prepared according to the Experimental Section contains approximately 1 water molecule for every 336 1-MN molecules based on the solubility of water in 1-MN.[54] (The solubility of 1-MN in water is much lower; 1 1-MN to ~2.6 × 10^5 H$_2$O.[61,62]) However, the Raman spectrum of the water-saturated 1-MN and the neat 1-MN are indistinguishable from each other, as observed by comparing the Raman spectra in Figure 2a and b. (We have also obtained Raman spectra in the OH bonding regions and do not observe any contribution from these regions of the spectrum from water absorption.) Yet, the surface BBSFG spectrum shows a dramatic change upon saturation of 1-MN with water, as observed by comparing the BBSFG spectra in Figure 2a and b. The BBSFG peak positions and their vibrational assignments shown within the Figure 2 insets are unaffected, yet a change in the relative peak areas is observed; therefore, the peaks assignments are the same as those for the neat 1-MN BBSFG spectrum shown in Figure 2a. As expected, the phase of the peaks and the nonresonant response remain unaffected upon water saturation. However, the peak areas of methyl peaks observed at 2908 cm^{-1} (CH$_3$ SS) and 2967 cm^{-1} (CH$_3$ AS) are enhanced, whereas the peak area of the aromatic CH stretch at 3063 cm^{-1} has decreased.

As revealed from Figure 2b, the water saturation of the 1-MN solution affects the orientation of the 1-MN molecules at the surface, with undetectable spectroscopic effects to the bulk liquid as demonstrated by the BBSFG and the Raman spectra shown in Figure 2a and b. The increased CH$_3$ SS and CH$_3$ AS peak areas in the SSP-polarized BBSFG spectrum from Figure 2b reveal an increased SFG response from the methyl groups at the surface of the water-saturated 1-MN solution. This indicates an increased surface number density of the CH$_3$ groups at the air−liquid interface where the methyl groups on neighboring surface 1-MN molecules are adjacent to one another on the same side of the adjacent rings, as shown in the schematic of Figure 3b. The result observed in Figure 2b also suggests that the 1-MN molecules do not lie flat in the interface. On average, there is some tilt angle associated with the plane of this molecule relative to the surface plane. The CH$_3$ AS peak area has also increased

1-Methyl Naphthalene Reorientation

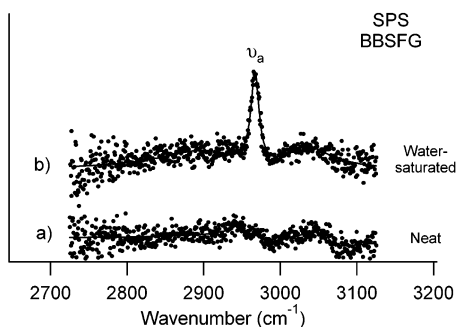*J. Phys. Chem. B, Vol. 107, No. 39, 2003* **10827**

Figure 4. Surface SPS BBSFG spectra of (a) neat 1-methyl naphthalene and (b) water-saturated 1-methyl naphthalene. The only discernible peak is the asymmetric stretching mode of the methyl group and is shown in b.

Figure 5. Surface SSP BBSFG spectra of (a) neat 1-methyl naphthalene, (b) partially hydrated 1-methyl naphthalene, and (c) water-saturated 1-methyl naphthalene.

to the approximate extent that is observed for the CH_3 SS peak area as shown in the inset of Figure 2b. This implies that the average distribution of the tilt angles of the surface 1-MN molecules of the water-saturated solution is similarly tilted relative to the surface normal as compared to the surface 1-MN molecules of the neat 1-MN solution. The SFG response of the CH_3 SS is expected to be enhanced if the 1-MN molecules are stacked as shown in Figure 3b. The methyl groups point toward the gas phase as indicated by the decrease in the aromatic CH peak upon water saturation of the 1-MN.

To elucidate the change in the surface structure further, surface tension (ST) measurements were performed on both the neat 1-MN and the water-saturated 1-MN solution. The surface tension was measured by the Wilhelmy method (Kibron Inc.). The ST of neat water at 28 °C was extrapolated from published values and calculated to be 71.5 ± 0.1 mN/m.[63] The ST of the neat 1-MN solution at 28 °C was found to be 30.6 ± 0.1 mN/m, and the ST of the water-saturated 1-MN at 28 °C was 30.8 ± 0.1 mN/m. The introduction of water into the 1-MN results in a small increase in the ST, indicating that water molecules have partitioned to the surface region. In addition, the rearrangement of the surface 1-MN molecules may also contribute to the increase in surface tension as a result of water saturation.

To investigate further the orientation of the surface 1-MN molecules of the water-saturated solution relative to the neat 1-MN liquid, additional BBSFG spectra were acquired using the $S_{SFG}P_{vis}S_{IR}$ polarization combination. The surface SPS BBSFG spectra of both the water-saturated 1-MN and the neat 1-MN solutions were collected, and the resultant spectra are shown in Figure 4. The surface spectrum of the water-saturated 1-MN solution (Figure 4b) has one well-resolved peak at 2970 cm^{-1} that is attributed to the CH_3 AS, consistent with the SSP BBSFG data, whereas the spectrum of the neat 1-MN (Figure 4a) is somewhat featureless with a relatively small SFG response from the CH_3 AS.

Recall that the transition moment of the CH_3 SS is along the methyl group's central axis and a component of the transition moment of the CH_3 AS is perpendicular to the methyl group's central axis. The SPS polarization combination contains s-polarized infrared light relative to the surface plane, which means that the electric field vector for the infrared beam is in the plane of the surface and the infrared light interacts efficiently with modes that have components in the plane of the surface. The enhancement of only the CH_3 AS mode using SPS-polarized BBSFG and the lack of response for the CH_3 SS strongly suggest that the CH_3 groups of the surface 1-MN molecules from the water-saturated solution are preferentially aligned with an average distribution that lies closer to the surface normal relative to the surface 1-MN molecules from the neat 1-MN liquid. This
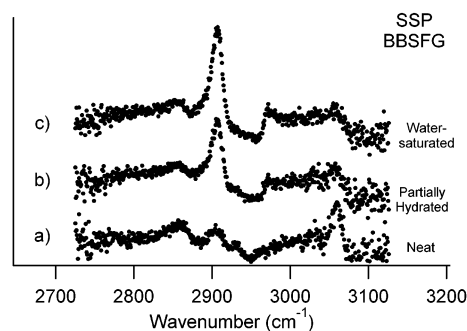
reorientation of the 1-MN surface molecules has clearly occurred after water saturation of the 1-MN solution even though the water content is relatively small, as indicated by the small increase in surface tension. The SPS result also supports the increase in the CH_3 surface number density.

The BBSFG $S_{SFG}S_{vis}P_{IR}$ polarization spectrum was also obtained for a partially dehydrated water-saturated 1-MN solution to elucidate this reorientation phenomenon further. The SSP BBSFG spectra of this solution along with SSP BBSFG spectra from the neat 1-MN liquid and water-saturated 1-MN solution are shown in Figure 5. Figure 5a shows the SSP BBSFG spectrum from the neat 1-MN liquid. Figure 5b shows the SSP BBSFG spectrum from the water-saturated 1-MN solution after partial dehydration, and Figure 5c shows the SSP BBSFG spectrum from the water-saturated 1-MN solution. The BBSFG peak areas of the CH_3 SS and the CH_3 AS observed at 2908 and 2967 cm^{-1}, respectively, for the partially dehydrated water-saturated spectrum (Figure 5b) are larger than these peaks observed from the spectrum in the neat 1-MN liquid (Figure 5a) and smaller than these peaks observed in the spectrum of the fully hydrated 1-MN solution (Figure 5c). However, the CH aromatic stretching vibration observed at 3063 cm^{-1} is smaller than the CH aromatic peak observed from the spectrum of the neat 1-MN (Figure 5a) and is slightly larger than the peak observed in the spectrum from the water-saturated 1-MN solution (Figure 5c).

As observed in Figure 5, the increase of the peak area from the aromatic CH stretching mode and the reduction of the peak area from the methyl stretching modes upon partial dehydration of the water-saturated 1-MN solution clearly indicate that the water-saturation process is reversible for 1-MN solutions. (The solution was first water-saturated and then partially dehydrated as described in the Experimental Section.) Although the BBSFG peak areas of the observed peaks change with the level of water saturation, frequency shifts are not observed; this confirms that the water has not reacted with the 1-MN molecules, yet interactions with the water molecules and the 1-MN molecules have occurred, as evidenced by the reorientation. Furthermore, it is clear from the observations in Figure 5a−c that the level of water saturation of the 1-MN solution influences the extent of the CH_3 orientation of the surface 1-MN molecules.

Conclusions

In summary, we have elucidated the surface structure of neat 1-methyl naphthalene (1-MN) and water-saturated 1-MN liquids using broad bandwidth sum frequency generation (BBSFG) spectroscopy, SSP- and SPS-polarized, in addition to the bulk structure of 1-MN using Raman spectroscopy. Surface tension measurements have also been utilized to probe the macroscopic

changes upon saturation of 1-MN with water and reveal that small amounts of water exist within the surface region. The 1-MN molecules at the surface of the neat 1-MN liquid have their aromatic rings aligned antiparallel to one another with their methyl groups alternating out of the surface and into the subsurface region from molecule to molecule. With the introduction of relatively few water molecules into the 1-MN liquid (1:336 water/1-MN), a rearrangement of the surface 1-MN molecules is induced, leading to an increased number density of the methyl groups arranged such that more methyl groups are oriented with their central axis pointing into the air phase at the air−liquid 1-MN interface. The reduction of the aromatic CH stretching peak area after water saturation further confirms that the preferred orientation of the surface 1-MN molecules has the majority of the methyl groups aligned on the air side of the interface. This reorientation of the molecules at the 1-MN surface is reversible through dehydration of the water-saturated 1-MN solutions. Clearly, water causes the reorientation of 1-MN surface molecules. Currently, we are investigating this reorientation phenomenon with several other aromatic hydrocarbon molecules at their respective air−liquid interfaces.

References and Notes

(1) Kolb, C. E.; Davidovits, P.; Jayne, J. T.; Shi, Q.; Worsnop, D. R. *Prog. React. Kinet. Mech.* **2002**, *27*, 1.

(2) Boniface, J.; Shi, Q.; Li, Y. Q.; Cheung, J. L.; Rattigan, O. V.; Davidovits, P.; Worsnop, D. R.; Jayne, J. T.; Kolb, C. E. *J. Phys. Chem. A* **2000**, *104*, 7502.

(3) Gershenzon, M.; Davidovits, P.; Jayne, J. T.; Kolb, C. E.; Worsnop, D. R. *J. Phys. Chem. A* **2001**, *105*, 7031.

(4) Nathanson, G. M.; Davidovits, P.; Worsnop, D. R.; Kolb, C. E. *J. Phys. Chem.* **1996**, *100*, 13007.

(5) Zhang, H. Z.; Li, Y. Q.; Davidovits, P.; Williams, L. R.; Jayne, J. T.; Kolb, C. E.; Worsnop, D. R. *J. Phys. Chem. A*, in press, 2003.

(6) Li, Y. Q.; Zhang, H. Z.; Davidovits, P.; Jayne, J. T.; Kolb, C. E.; Worsnop, D. R. *J. Phys. Chem. A* **2002**, *106*, 1220.

(7) Arey, J.; Atkinson, R.; Zielinska, B.; McElroy, P. A. *Environ. Sci. Technol.* **1989**, *23*, 321.

(8) Fraser, M. P.; Cass, G. R.; Simoneit, B. R. T.; Rasmussen, R. A. *Environ. Sci. Technol.* **1998**, *32*, 1760.

(9) Schauer, J. J.; Kleeman, M. J.; Cass, G. R.; Simoneit, B. R. T. *Environ. Sci. Technol.* **2002**, *36*, 1169.

(10) Fraser, M. P.; Kleeman, M. J.; Schauer, J. J.; Cass, G. R. *Environ. Sci. Technol.* **2000**, *34*, 1302.

(11) Hawthorne, S. B.; Grabanski, C. B. *Environ. Sci. Technol.* **2000**, *34*, 4348.

(12) Fraser, M. P.; Cass, G. R.; Simoneit, B. R. T. *Environ. Sci. Technol.* **1998**, *32*, 2051.

(13) Forstner, H. J. L.; Flagan, R. C.; Seinfeld, J. H. *Environ. Sci. Technol.* **1997**, *31*, 1345.

(14) Smith, D. J. T.; Harrison, R. M. In *Atmospheric Particles*; Harrison, R. M., Ed.; IUPAC Series on Analytical and Physical Chemistry; Wiley & Sons: Chichester, England, 1998; Vol. 5, p 253.

(15) Wingfors, H.; Sjodin, A.; Haglund, P.; Brorstrom-Lunden, E. *Atmos. Environ.* **2001**, *35*, 6361.

(16) Shihua, Q.; Jun, Y.; Gan, Z.; Jiamo, F.; Guoying, S.; Zhishi, W.; Tong, S. M.; Tang, U. W.; Yunshun, M. *Environ. Monit. Assess.* **2001**, *72*, 115.

(17) Kado, N. Y.; Okamoto, R. A.; Kuzmicky, P. A.; Rathbun, C. J.; Hsieh, D. P. H. *Chemosphere* **1996**, *33*, 495.

(18) Siegl, W. O.; Hammerle, R. H.; Herrmann, H. M.; Wenclawiak, B. W.; Luers-Jongan, B. *Atmos. Environ.* **1999**, *33*, 797.

(19) Rhead, M. M.; Pemberton, R. D. *Energy Fuels* **1996**, *10*, 837.

(20) Short, J. W.; Heintz, R. A. *Environ. Sci. Technol.* **1997**, *31*, 2375.

(21) Sauer, T. C.; Michel, J.; Hayes, M. O.; Aurand, D. V. *Environ. Int.* **1998**, *24*, 43.

(22) Finlayson-Pitts, B. J.; Pitts, J. N., Jr. *Chemistry of the Upper and Lower Atmosphere: Theory, Experiments and Applications*; Academic Press: San Diego, CA, 2000.

(23) Day, M. *New Sci.* **1998**, *158*, 23.

(24) Dockery, D. W.; Pope, C. A.; Xu, X. P.; Spengler, J. D.; Ware, J. H.; Fay, M. E.; Ferris, B. G.; Speizer, F. E. *N. Engl. J. Med.* **1993**, *329*, 1752.

(25) Li, N.; Wang, M. Y.; Oberley, T. D.; Sempf, J. M.; Nel, A. E. *J. Immunol.* **2002**, *169*, 4531.

(26) Yin, X. J.; Schafer, R.; Ma, J. Y. C.; Antonini, J. M.; Weissman, D. D.; Siegel, P. D.; Barger, M. W.; Roberts, J. R.; Ma, J. K. H. *Environ. Health Perspect.* **2002**, *110*, 1105.

(27) Gupta, P.; Harger, W. P.; Arey, J. *Atmos. Environ.* **1996**, *30*, 3157.

(28) Atkinson, R.; Arey, J. *Environ. Health Perspect.* **1994**, *102*, 117.

(29) Ma, G.; Allen, H. C. *J. Am. Chem. Soc.* **2002**, *124*, 9374.

(30) Lambert, A. G.; Neivandt, D. J.; Briggs, A. M.; Usadi, E. W.; Davies, P. B. *J. Phys. Chem. B* **2002**, *106*, 5461.

(31) Miranda, P. B.; Shen, Y. R. *J. Phys. Chem. B* **1999**, *103*, 3292.

(32) Eisenthal, K. B. *Chem. Rev.* **1996**, *96*, 1343.

(33) Richmond, G. L. *Chem. Rev.* **2002**, *102*, 2693.

(34) Shultz, M. J.; Schnitzer, C.; Simonelli, D.; Baldelli, S. *Int. Rev. Phys. Chem.* **2000**, *19*, 123.

(35) Ward, R. N.; Duffy, D. C.; Bell, G. R.; Bain, C. D. *Mol. Phys.* **1996**, *88*, 269.

(36) Hommel, E. L.; Allen, H. C. *Analyst (Cambridge, U.K.)* **2003**, *28*, 750.

(37) Allen, H. C.; Raymond, E. A.; Richmond, G. L. *Curr. Opin. Colloid Interface Sci.* **2000**, *5*, 74.

(38) Allen, H. C.; Raymond, E. A.; Richmond, G. L. *J. Phys. Chem. A* **2001**, *105*, 1649.

(39) Ma, G.; Allen, H. C. *J. Phys. Chem. B* **2003**, *107*, 6343.

(40) Simonelli, D.; Baldelli, S.; Shultz, M. J. *Chem. Phys. Lett.* **1998**, *298*, 400.

(41) Shultz, M. J.; Baldelli, S.; Schnitzer, C.; Simonelli, D. *J. Phys. Chem. B* **2002**, *106*, 5313.

(42) Raduge, C.; Pflumio, V.; Shen, Y. R. *Chem. Phys. Lett.* **1997**, *274*, 140.

(43) Shen, Y. R. *The Principles of Nonlinear Optics*, 1st ed.; Wiley & Sons: New York, 1984.

(44) Bain, C. D. *J. Chem. Soc., Faraday Trans.* **1995**, *91*, 1281.

(45) Wolfrum, K.; Laubereau, A. *Chem. Phys. Lett.* **1994**, *228*, 83.

(46) Dick, B.; Gierulski, A.; Marowsky, G. *Appl. Phys. B* **1985**, *38*, 107.

(47) Morita, A.; Hynes, J. T. *Chem. Phys.* **2000**, *258*, 371.

(48) Hirose, C.; Yamamoto, H.; Akamatsu, N.; Domen, K. *J. Phys. Chem.* **1993**, *97*, 10064.

(49) Hirose, C.; Akamatsu, N.; Domen, K. *J. Chem. Phys.* **1992**, *96*, 997.

(50) Hirose, C.; Akamatsu, N.; Domen, K. *Appl. Spectrosc.* **1992**, *46*, 1051.

(51) Hunt, J. H.; Guyot-Sionnest, P.; Shen, Y. R. *Chem. Phys. Lett.* **1987**, *133*, 189.

(52) Hommel, E. L.; Allen, H. C. *Anal. Sci.* **2001**, *17*, 137.

(53) Hommel, E. L.; Ma, G.; Allen, H. C. *Anal. Sci.* **2001**, *17*, 1325.

(54) Englin, B. A.; Plate, A. F.; Tugolukov, V. M.; Pryanishnikova, M. A. *Khim. Tekhnol. Topl. Masel* **1965**, *10*, 42.

(55) Morrison, V. J.; Laposa, J. D. *Spectrochim. Acta, Part A* **1976**, *32*, 443.

(56) Balfour, W. J.; Fried, Y. *Can. J. Chem.* **1994**, *72*, 1218.

(57) Fox, J. J.; Martin, A. E. *J. Chem. Soc.* **1939**, 318.

(58) Galli, J.; Fruwert, J.; Geiseler, G. *Z. Chem.* **1976**, *16*, 57.

(59) Brown, M. G.; Raymond, E. A.; Allen, H. C.; Scatena, L. F.; Richmond, G. L. *J. Phys. Chem. A* **2000**, *104*, 10220.

(60) Drozdowski, H. *Chem. Phys. Lett.* **2002**, *351*, 53.

(61) Mackay, D.; Shiu, W. Y. *J. Phys. Chem. Eng. Data* **1977**, *22*, 399.

(62) Schwarz, F. P. *J. Chem. Eng. Data* **1977**, *22*, 273.

(63) Vazquez, G.; Alvarez, E.; Navaza, J. M. *J. Chem. Eng. Data* **1995**, *40*, 611.